Appl. Phys. B 50, 371–379 (1990)

Applied Physics B Photophysics and Laser Chemistry

C_2 Creation, Emission, and Laser-Induced Fluorescence in Flames and Cold Gases*

J. E. M. Goldsmith and D. Therese Biernacki Kearsley**

Combustion Research Facility, Sandia National Laboratories, Livermore, CA 94551, USA

Received 27 October 1989/Accepted 6 January 1990

Abstract. We describe photochemical production of C_2 in the upper ($d^3\Pi_g$) and the lower ($a^3\Pi_u$) levels of the Swan-band transitions by 266 and 292-nm laser irradiation of flames and room-temperature flows of acetylene and ethylene. Topics treated include the spectroscopy of the Swan bands, lifetimes and quenching of the Swan-band emission, intensity dependences of the Swan-band emission in several environments, profiles of C_2 in low-pressure hydrocarbon flames, and the affect of Swan-band emission on three-photon-excited fluorescence detection of atomic hydrogen in hydrocarbon flames.

PACS: 33.80.Wz, 82.40.Py, 82.50.Fv

The Swan bands of the C_2 molecule ($d^3\Pi_g - a^3\Pi_u$ transitions in the range 400–600 nm) appear frequently in the spectroscopic literature. These bands give rise to the rich blue-green emission evident in hydrocarbon flames, and have long been studied in flame emission spectroscopy [1]. Their convenient wavelengths have been exploited for a variety of laser-based measurements of C_2 in flames. In a different vein, C_2 Swan-band emission seems to be ubiquitous in many environments, appearing almost any time that intense laser pulses, with wavelengths anywhere through the visible to the vacuum-ultraviolet regions of the spectrum, irradiate carbon-containing compounds. In this paper, we attempt to characterize the laser-induced creation of Swan-band emission in cold gases and flames, and to discuss the impact of these processes on some laser-induced fluorescence measurements in flames, particularly three-photon-excited fluorescence detection of atomic hydrogen [2].

Classical flame absorption and emission measurements of C_2 are described in [1]. Laser excitation of the Swan bands have been used in several flame studies, first relying on the accidental coincidence between the 514-nm line from the argon-ion laser and transitions in the (0, 0) Swan band [3], and then using a tunable dye laser [4]. Later refinements include saturated fluorescence measurements [5, 6], intracavity tomographic [7] and fluorescence [8] measurements, one- [9] and two-dimensional [10, 11] fluorescence imaging, and coherent anti-Stokes Raman spectroscopy (CARS) studies [12, 13]. In a separate class of studies, Swan-band emission has been observed in many experiments involving irradiation of carbon-containing solids and gases with intense laser pulses, even though the sample may not contain any nascent C_2 and the laser wavelength is not resonant with any single- or multiphoton resonances of C_2. Analysis of Swan-band emission created by focusing a laser beam onto a graphite block was reported shortly after the invention of the laser [14]. Multiphoton infrared [15] and ultraviolet [16] processes leading to Swan-band emission have also been described.

Swan-band emission from laser-created C_2 has also been shown to affect directly several laser-based combustion diagnostic techniques. Swan-band interferences can directly affect CARS measurements made in sooting flames [17]. In a study of simultaneous fluorescence imaging of C_2 and OH in flames, use of a

* This work was supported by the U.S. Department of Energy, Office of Basic Energy Sciences, Division of Chemical Sciences

** Sandia Postdoctoral Research Associate. Current address: Molecular Design Ltd.; 2200 Route 10, Executive 10; Parsippany, NJ 07054, USA

309-nm laser beam to excite OH fluorescence did not create measurable quantities of C_2, but use of a 282-nm beam did create significant quantities of C_2 (not resonant with the OH transitions) [9]. In two-photon-excited fluorescence studies of CO using a 230-nm laser beam, strong Swan-band emission was produced, even when the sample was pure CO in a cell; unlike the previous 282-nm case, in the CO study the C_2 emission was primarily resonant with the CO two-photon excitation process [18]. Interferences with fluorescence [19] and Raman [20] measurements caused by creation of C_2 by multiphoton processes using visible laser wavelengths in nonsooting regions of diffusion flames have also been described.

In this paper, we first describe the experimental apparatus used for the C_2 studies. We next describe the spectroscopy of the Swan bands, illustrating it with laser excitation and resolved emission spectra. The temporal behavior of the emission pulses is described next, followed by a description of the intensity dependences observed for the photolytic creation process in cold gases and under flame conditions. The final sections of the paper describe profile measurements of nascent and created C_2 in flames, and discuss the impact of Swan-band emission on fluorescence detection of other species. Three excitation wavelengths were used in these studies. Laser-induced fluorescence measurements of the (0, 0) rovibronic transitions of the Swan bands were made using 517-nm radiation. Photochemical creation studies were performed using both 266 and 292-nm radiation; the former was chosen because of the ease with which it can be generated, and the latter was chosen because it is used for three-photon-excited fluorescence measurements of atomic hydrogen in flames [2].

1. Experimental Apparatus

Three excitation wavelengths, 517, 292, and 266 nm, were used for the measurements described in this paper. Tunable 517-nm radiation was produced by using the 355-nm third-harmonic output from a Quanta-Ray DCR-2A Nd:YAG laser to pump a Quanta-Ray PDL-2 dye laser with Coumarin 500 dye. Tunable 292-nm radiation, used for three-photon excitation of atomic hydrogen [2, 21] and C_2 creation studies, was produced by using the 532-nm second-harmonic output from a Quantel 581-C Nd:YAG laser to pump either a Quanta-Ray PDL-1 dye laser (0.25 cm^{-1} nominal bandwidth) or a Lumonics HyperDYE-300 laser (0.08 cm^{-1} nominal bandwidth), both operated with Kiton Red dye, and subsequently frequency-doubled by a Quanta-Ray WEX-1 wavelength extender. Fixed-wavelength 266-nm radiation ($\sim$0.1 cm^{-1} bandwidth), used for C_2 creation studies, was produced by frequency-doubling the 532-nm output of the Quanta-Ray DCR-2A Nd:YAG laser by a second WEX-1 wavelength extender, using the C-7 83° KDP crystal in the CM-2 crystal module in the location normally occupied by the CM-1 module. This scheme made it possible to use the active crystal-angle stabilization provided by the WEX to produce the fourth-harmonic Nd:YAG wavelength, avoiding the long-term power instabilities generally associated with fourth-harmonic operation. The pulse energy focused into the flame chamber was controlled using a Newport Corporation Model 935-10 variable attenuator, and the energy of each pulse was measured by placing an uncoated beamsplitter after the flame chamber and reflecting a fraction of the beam into a Molectron Detector Inc. Model J3-09 pyroelectric Joulemeter. The output of the Joulemeter was calibrated by measuring the pulse energy of the full beam with Scientech Model 38-0103 and 38-0105 energy meters.

All measurements were performed using a vacuum chamber designed for operation with low-pressure flames. Premixed gases, with flows controlled by Tylan flow controllers, entered the chamber and flowed through the center section of a McKenna Inc. 6-cm-diameter flat-flame burner, which was mounted on a computer-controlled micrometer stage for measuring vertical flame profiles. This center section consists of a porous plug of sintered material; burners containing bronze and stainless-steel center sections were used. The pressure in the chamber was monitored and controlled by an MKS control system. The flow characteristics of the flames we investigated are summarized in Table 1; most of these flames were chosen because they have been used in other studies ([21] and references therein). The same apparatus was used for the cold-gas (room temperature) measurements described in this paper, maintaining gas flow rates sufficient to ensure fresh packets of gas for each laser pulse to avoid build-up of photolysis byproducts.

Table 1. Flames investigated in this study

Equivalence ratio	Pressure [Torr]	Fuel [l/min]	Oxidant [l/min]	Diluent [l/min]
0.6	30	CH_4(1.5)	O_2(5.3)	–
1.6	30	CH_4(3.0)	O_2(3.8)	–
1.2	30	C_2H_4(1.5)	O_2(3.8)	–
1.0	30	C_2H_2(0.2)	O_2(0.5)	Ar(3.9)
1.6	25	C_2H_2(1.1)	O_2(1.7)	Ar(7.0)
1.8	25	C_2H_2(1.2)	O_2(1.7)	Ar(6.2)
2.0	25	C_2H_2(1.4)	O_2(1.7)	Ar(6.2)
2.4	25	C_2H_2(1.6)	O_2(1.7)	Ar(0.7)

Standard-grade gases (H_2, CH_4, C_2H_2, C_2H_4, O_2, and Ar) were used for all measurements. Analysis of gas from the acetylene cylinder indicated 98.1% C_2H, 1.82% acetone (stabilizer), 0.05% H_2, 0.02% O_2, and 0.01% C_4 and C_5 hydrocarbons. The acetylene was filtered by an activated charcoal filter (Matheson 454), but no further gas purification measures were taken.

Swan-band emission from the laser-excited gases was monitored by two detection systems. For most of the studies, the emission was filtered by a 560-nm interference filter (9 nm bandwidth FWHM), which transmitted radiation in the $\Delta v = -1$ bands [(0,1), (1,2), etc.; the values (v', v'') refer to the vibrational levels of the upper (v') and the lower (v'') electronic states]. Resolved-emission spectra were recorded using a Spex Model 1870-C 0.5-m spectrometer. For both systems, the transmitted radiation was monitored by a Hamamatsu R-955 photomultiplier, with the output pulses amplified by a Comlinear E-103 video amplifier. Most measurements were made using a Stanford Research Systems SR-250 gated integrator to integrate the emission signal, followed by analog-to-digital conversion for subsequent processing by the DEC MicroVAX II microcomputer that controlled the experiment. Measurements of the temporal decay profile of the pulses were made using a LeCroy Model 9400 digital oscilloscope, operated using random-interleave sampling and 10-trace averaging. Using a Hamamatsu Model C1308 pulser (pulse duration <1 ns), we measured an instrument-limited exponential fall time of 8 ns and a rise time of 2 ns, capable of resolving all but the fastest decays observed in our studies.

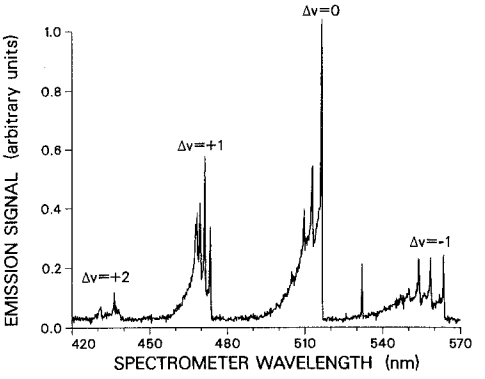

Fig. 1. Spectrum of the resolved Swan-band emission produced by irradiating a 25-Torr acetylene-oxygen-argon flame stabilized on the bronze burner with 292-nm laser pulses and recorded using the Spex spectrometer with 200-μm slits. The peak at 532 nm is from scattered frequency-doubled Nd:YAG-laser radiation

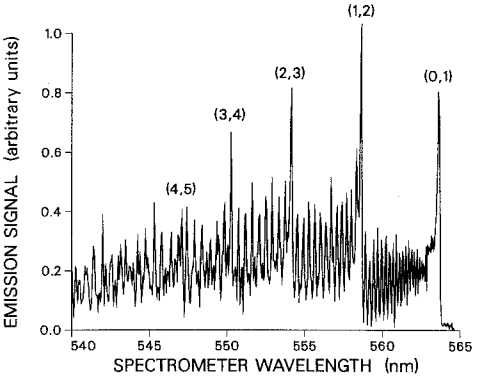

Fig. 2. Spectrum of the resolved Swan-band emission ($\Delta v = -1$ progression) produced by irradiating a 25-Torr sample of room-temperature acetylene with 266-nm, 22-mJ laser pulses and recorded using the Spex spectrometer with 50-μm slits

2. Spectroscopy

The Swan bands arise from transitions between the $a^3\Pi_u$ and $d^3\Pi_g$ electronic states of the C_2 molecule. The $a^3\Pi_u$ state was originally believed to be the lowest-lying electronic state of the molecule, causing the $a^3\Pi_u$ and $d^3\Pi_g$ states to be labeled $X^3\Pi_u$ and $A^3\Pi_g$ in early literature [22]; the $a^3\Pi_u$ state in fact lies 716 cm^{-1} above the true $X^1\Sigma_g^+$ ground state [23]. The broad structure of the Swan-band emission is shown in Fig. 1. This spectrum was recorded by irradiating a 25-Torr, equivalence ratio 2.4 (fuel-rich) acetylene-oxygen-argon flame with 15-mJ, 292-nm laser pulses, and resolving the laser-induced C_2 emission at relatively low resolution ($\sim$0.6 nm FWHM) with the Spex spectrometer. The rotational structure of the $\Delta v = -1$ progression is shown at higher resolution ($\sim$0.15 nm FWHM) in Fig. 2, recorded by irradiating a 25-Torr flow of room-temperature acetylene with 20-mJ, 266-nm pulses. We did not see any indication of enhanced emission from $v' = 6$ levels in any of our studies. This enhanced emission, called the "high-pressure" Swan band, is most commonly associated with observations of Swan-band emission using carbon monoxide as a photochemical precursor, and is generally not observed using other simple gases as precursors [24].

3. Temporal Dependence

Recent measurements of radiative lifetimes for the upper levels of the Swan-band transitions ($d^3\Pi_g$ states) report values of 92–106 ns, although a series of previous measurements gave values of 120 ± 10 ns [25]. We did not make any measurements in collision-free environments, but instead studied the temporal behavior of the laser-induced C_2 emission in a variety of flames and mixtures of room-temperature gases. Figure 3 displays a typical measurement, recorded in a

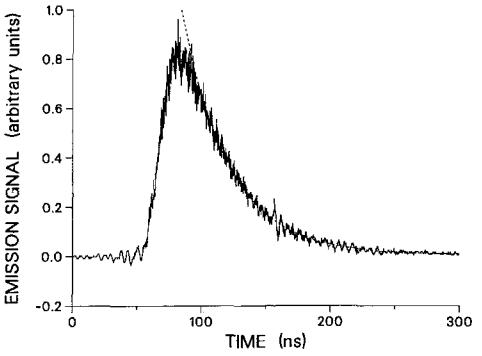

Fig. 3. Time dependence of the Swan-band emission produced by irradiating a 5-Torr sample of room-temperature ethylene with 292-nm laser pulses and monitoring the 517-nm emission with the Spex spectrometer (solid curve), and least-squares fit of the decay portion to an exponential (dashed curve)

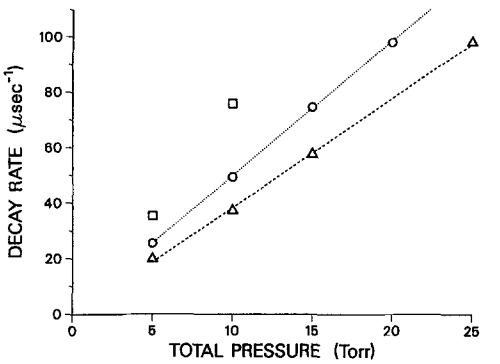

Fig. 4. Decay rates of Swan-band emission produced by 292-nm irradiation and 517-nm Spex spectrometer detection in room-temperature flows of acetylene (triangles, ~5 mJ/pulse) and ethylene (circles, ~5 mJ/pulse; squares, ~25 mJ/pulse) at total pressures from 5–25 Torr

5-Torr flow of ethylene irradiated by 292-nm pulses, and monitoring the $\Delta v=0$, 517-nm progression using the Spex spectrometer operated with 400-μm slits (0.8-nm FWHM resolution). The prompt emission, evident from the rapid rise of the signal observed in all of our measurements, indicates that $d^3\Pi_g$ molecules are direct photolysis products (creation via a chemical reaction mechanism would occur on a much longer time scale, resulting in a longer signal rise time). The dashed line represents a least-squares fit to an exponential decay of the signal in the range 100–300 ns, with a resulting decay time of 37 ns. Studying various gas mixtures and pressures, we observed decay rates as slow as 90 ns in a 5-Torr mixture of acetylene and argon, and 75 ns in a 20-Torr acetylene-oxygen-argon flame, as well as rates as fast as our instrument-limited detection rate (8 ns).

We measured the laser-excited C_2 emission rate as a function of pressure in room-temperature flows of acetylene and ethylene to obtain information about the collisional quenching rates of the Swan-band transitions. As described for Fig. 3, these measurements were performed by irradiating the flowing gas with 292-nm pulses, and monitoring the $\Delta v=0$, 517-nm progression using the Spex spectrometer operated with 400-μm slits (0.8-nm FWHM resolution). The results are shown in Fig. 4. The dashed line represents the best-fit line through the triangles representing the data set for acetylene, with a slope of 3.9 $\mu s^{-1}\,Torr^{-1}$. The dotted line represents the best-fit line through the circles representing the lower-intensity data set (~5 mJ/pulse) for ethylene, with a slope of 4.8 $\mu s^{-1}\,Torr^{-1}$.

Measurements made in ethylene at higher 292-nm pulse energies (~25 mJ/pulse) yielded the two points represented by the squares; the measured rates are clearly faster than the lower-energy data set (circles). This increase in decay rate with increase in pulse energy may be due to the creation of significant quantities of photochemically created byproducts (the electronically excited C_2 is itself a photochemical byproduct), which evidently quench the Swan-band emission at a higher rate than the parent ethylene gas. It should be pointed out that these results are of limited utility, even without this apparent intensity dependence, because the rovibronic distribution of electronically excited C_2 molecules, and hence the effective quenching rate, is likely to depend on many details of the photochemical creation mechanism and the collisional environment. Collisional energy transfer from C_2 created in other electronic states can affect decay rates measured at elevated pressures of the precusor gas or other collision partners [26], and some buffer gases can enhance Swan-band emission under the appropriate conditions [27].

4. Intensity Dependences

Intensity dependences can provide important mechanistic information on multiphoton processes; we have used such information in studying photochemical formation of atomic hydrogen [28, 29] and oxygen [30] occurring during multiphoton excitation studies of these atomic species in flames. "Intensity dependence" refers to the power of the laser intensity to which the observed signal is proportional, i.e., the value of "n" in signal$\propto I^n$, usually derived from a log-log plot of signal versus intensity. We describe here similar measurements for photochemical creation of electronically excited C_2, observed by monitoring the laser-induced Swan-band emission as a function of incident pulse energy. We present results which illustrate the effects of varying excitation wavelength (266

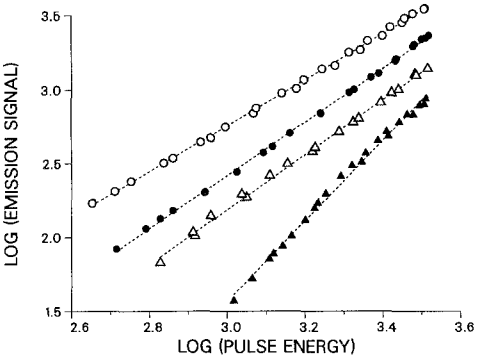

Fig. 5. Intensity dependences of Swan-band emission observed using the 560-nm interference filter in the detection channel by irradiating 25-Torr, room-temperature flows of acetylene (open symbols) and ethylene (filled symbols) with laser pulses up to 20 mJ/pulse focused by a 50-cm focal-length lens at 266 nm (circles) and 292 nm (triangles)

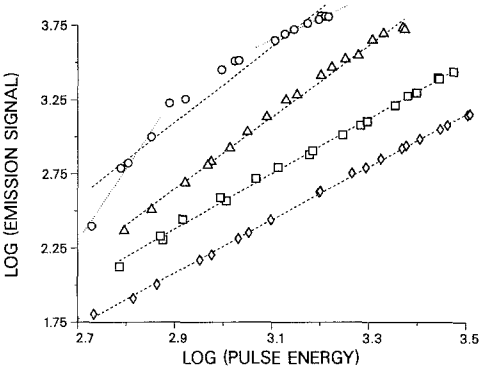

Fig. 6. Intensity dependences of Swan-band emission observed using the 560-nm interference filter in the detection channel by irradiation room-temperature flows of acetylene with 292-nm laser pulses at total pressures of 10 Torr (diamonds), 25 Torr (squares), 50 Torr (triangles), and 100 Torr (circles)

and 292 nm) in room-temperature hydrocarbon flows (acetylene and ethylene), gas pressure, and location in a flame (below and in the reaction zone). For each setting of the variable attenuator in the incident laser beam, the computer averaged the incident pulse energy and the emission signal for 200 consecutive laser pulses. The measurements described in this section were all reproducible, although the variations in the measured slopes of the log-log plots (typically ± 0.1–0.2) were somewhat larger than we have observed in studies of other species.

Figure 5 displays intensity dependences recorded in 25-Torr flows of room-temperature acetylene and ethylene, excited by 266 and 292-nm laser pulses. All measurements were made using a 50-cm focal-length lens to focus laser pulses with energies up to 20 mJ/pulse into the gas flow, and filtering the emission with the 560-nm interference filter. (Measurements made using the Spex spectrometer to isolate various vibrational sequences yielded the same results.) The dashed lines represent linear fits to the four data sets, yielding slopes of $n=1.6$ for acetylene and 266-nm radiation, $n=1.8$ for ethylene and 266-nm radiation, $n=1.9$ for acetylene and 292-nm radiation, and $n=2.7$ for ethylene and 292-nm radiation. It is tempting to conclude that these measurements suggest two-photon creation processes for the first three (acetylene at both wavelengths and ethylene at 266 nm), and a three-photon process for ethylene at 292 nm. However, if a transition of a multi-step process is saturated, the intensity dependence will indicate only the order of nonlinearity of the rate-limiting step, rather than the total number of photons involved in the process.

Previous measurements of intensity dependences of C_2 creation from acetylene used 193-nm radiation from ArF lasers. Two intensity dependences appear for creation of C_2 in the $d^3\Pi_g$ state, which is responsible for the Swan-band emission. McDonald et al. reported a value of $n=2.40\pm0.20$ measured in 30 mTorr of acetylene, interpreting this as indicating that the electronically excited C_2 fragments require the absorption of three photons [16]. Okabe et al. reported no observable differences using 20-mTorr samples of acetylene or CF_3C_2H and detecting the (1,0) or the (0,0) sequences, with a resulting intensity dependence of $n=1.53\pm0.07$; the discrepancy with the previous value is suggested as being due to the use of power densities at least twice as high, and thus possible saturation of an absorption step [31]. For creation of C_2 in the $a^3\Pi_u$ state, the lower level of the Swan-band transitions, Donnelly and Pasternack reported that laser power dependences indicate a two-photon formation mechanism, but did not give the actual value of the measured intensity dependence [32]. Wodtke and Lee ascribe creation of C_2 in the $a^3\Pi_u$ state and in the $X^1\Sigma_g^+$ ground electronic state as occurring primarily through sequential single-photon steps, $C_2H_2 \rightarrow C_2H + H$ followed by $C_2H \rightarrow C_2 + H$ [33].

Figure 6 shows similar measurements, all made using 292-nm pulses to irradiate room-temperature flows of ethylene, but at four different pressures. All measurements were made with the same range of pulse energies (up to 20 mJ/pulse), and are plotted to the same horizontal scale. Because the pulse energy is monitored after the flame chamber, significant absorption along the 30-cm path length in the chamber ($\sim 50\%$ at 100 Torr) shifts the curves to the left as the pressure increases, but does not change their slopes. As is evident from the dashed lines (linear fits to the full data sets), the slopes increase with increasing total pressure, from $n=1.8$ at 10 Torr to $n=1.9$ at 25 Torr, $n=2.4$ at 50 Torr, and $n=2.5$ at 100 Torr. The 10-Torr

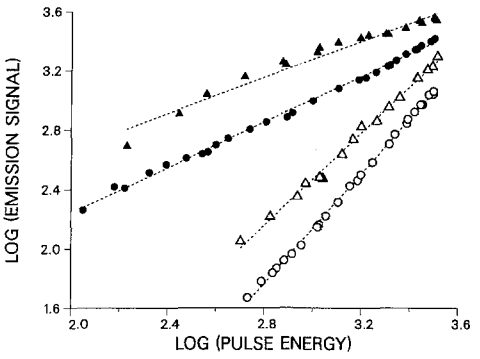

Fig. 7. Intensity dependences of Swan-band emission observed using the 560-nm interference filter in the detection channel by irradiating the 30-Torr, equivalence-ratio 1.0 acetylene-oxygen-argon flame stabilized on the stainless-steel burner with laser pulses at 266 nm (circles) and 292 nm (triangles), near the burner surface (open symbols) and at the peak of the profile 13 mm above the burner surface (filled symbols)

and 25-Torr data sets are quite linear, but a small amount of curvature is evident in the 50-Torr data set, and a great deal of curvature appears in the 100-Torr data set, with slopes (indicated by the dotted lines) varying from $n=4.9$ at the lower pulse energies to $n=1.5$ at the higher pulse energies. We are unable to explain this effect at this time.

Figure 7 displays four intensity dependences measured in a stoichiometric, 30-Torr acetylene-oxygen-argon flame, using a 50-cm focal-length lens to focus laser pulses with energies up to 20 mJ/pulse into the gas flow, and filtering the emission with the 560-nm interference filter. The data sets with open symbols were measured close to the burner surface before the reaction zone of the flame, and thus in relatively cool gases (a few hundred degrees above room temperature). The measurements made using 266-nm pulses (circles) and 292-nm pulses (triangles) have very similar slopes ($n=1.8$ and $n=1.6$, respectively), consistent with the room-temperature acetylene measurements shown in Fig. 5. The data sets with solid symbols were measured higher above the burner in the reaction zone, at the height which produced the largest Swan-band emission signal (profiles of this flame are presented in the following section of the paper). The measurements made using 266-nm pulses (circles) and 292-nm pulses (triangles) again have similar slopes ($n=0.8$ and $n=0.6$, respectively), but are not nearly as steep as the measurements made near the burner surface, and significant curvature is evident in the 292-nm data set (solid triangles). These changes in the intensity dependences are not unreasonable considering the changes in the local environment in which they were measured, going from an essentially room-temperature acetylene-oxygen-argon mixture to the hot reaction zone containing a variety of radicals in addition to stable species. The only intensity dependences measured in flames that we could find in the literature were both made using visible excitation wavelengths: 563-nm excitation created Swan-band emission via a multiphoton process in non-sooting regions of a methane/air diffusion flame [19], and 532-nm excitation using a much longer pulse from a flashlamp-pumped dye laser (3-μs pulse length) created Swan-band emission with a measured intensity dependence of $n=4$ in nonpremixed methane flames [20].

5. Flame Profiles

From the point of view of combustion diagnostics, the most interesting aspect of laser-induced Swan-band emission is the information it presents on species concentrations in flames, and how this emission can affect profile measurements of other flame species. To start exploring the former, we measured height profiles of the Swan-band emission signal for different excitation conditions in a variety of hydrocarbon flames. These studies provide information on the regions in the flame in which C_2 molecules are created in the electronically excited $d^3\Pi_g$ state. For comparison, we also measured laser-induced fluorescence profiles of the $a^3\Pi_u$ state (which lies 716 cm^{-1} above the ground $X^1\Sigma_g^+$ state) by exciting the (0, 0) band at 517 nm and detecting the (0, 1) fluorescence using the 560-nm interference filter.

A typical result of these types of studies is shown in Fig. 8. These profiles were measured in a 25-Torr, equivalence-ratio 2.0 acetylene-oxygen-argon flame using the stainless steel burner, and were normalized to a value of unity at their peaks. The circles show a 517-nm laser-induced fluorescence profile representing the distribution of the $a^3\Pi_u$ state. The triangles and squares show profiles representing laser-induced creation of Swan-band emission using 10-mJ 266-nm and 292-nm pulses, respectively. All profiles were measured using the 560-nm interference filter in the detection channel. The basic features of these profiles were observed in several of the hydrocarbon flames. In all cases, the creation peaks occurred at the same height above the burner for 266-nm and for 292-nm excitation, with those peaks located 1–2 mm closer to the burner than the 517-nm fluorescence peak. The "hump" in the 292-nm creation peak relative to the 266-nm peak in the region 7–13 mm above the burner was observed consistently in rich acetylene flames, but was not evident in a rich methane flame. Using the Spex spectrometer to isolate the emission in various rovibronic sequences (Fig. 1), we found that the shapes of the profiles were independent of detection band. We

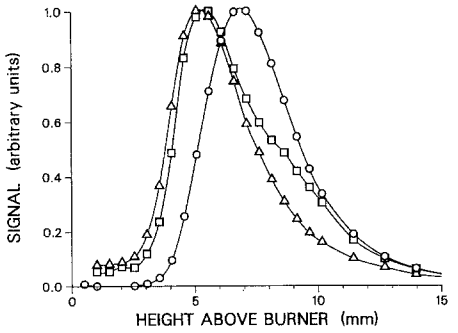

Fig. 8. Profiles recorded in the 25-Torr, equivalence-ratio 2.0 acetylene-oxygen-argon flame stabilized on the stainless-steel burner using the 560-nm interference filter in the detection channel. Circles: 517-nm-excited LIF profile. Triangles and squares: Laser-created Swan-band emission produced using 10-mJ laser pulses at 266-nm (triangles) and 292-nm (squares)

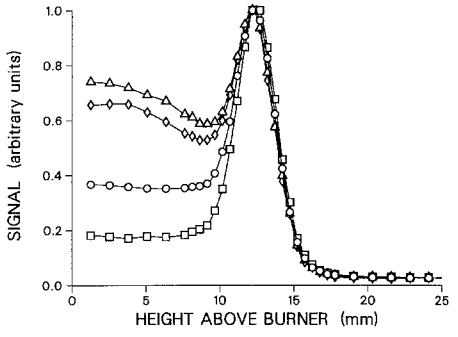

Fig. 9. Profiles of the Swan-band emission recorded in the 30-Torr, equivalence-ratio 1.0 acetylene-oxygen-argon flame stabilized on the stainless-steel burner using the 560-nm interference filter in the detection channel by irradiating the flame with 266-nm laser pulses of 5 mJ (squares), 10 mJ (circles), 20 mJ (diamonds), and 25 mJ (triangles). The four profiles have been normalized to match at their peaks

did not observe any laser-induced Swan-band emission in a lean methane-oxygen flame, and measured less emission in a rich methane-oxygen flame than in acetylene flames (not at all surprising considering that, like C_2, acetylene contains a carbon-carbon bond but methane does not).

Figure 9 illustrates the effect of variations in 266-nm pulse energy on Swan-band creation profiles measured in the 30-Torr, stoichiometric acetylene-oxygen-argon flame, again using the stainless-steel burner. These profiles were measured with pulse energies of 5 mJ (squares), 10 mJ (circles), 20 mJ (diamonds), and 25 mJ (triangles); the profiles are normalized to a value of unity at their peaks. Varying the pulse energy did not affect the shape of the main peak, but did change the magnitude of the peak relative to the signal near the burner surface. This behavior is consistent with the observation (discussed in reference to Fig. 7) that the intensity dependence of the signal at the peak is not as strong as the intensity dependence near the burner. This behavior was also observed in profiles measured in the rich acetylene flames, but was not nearly as pronounced because the signal near the burner was much smaller in relative magnitude to the signal at the peak of the profile over the range of pulse energies investigated.

Our initial flame measurements were performed using the bronze burner. We had used that burner for operating hydrogen and methane flames for many days without encountering any difficulties. After just a few days of operating acetylene flames, however, the sintered burner material developed regions that were partially or completely plugged, causing the flame to become very nonuniform, a difficulty we have been told is not unique. We encountered no further difficulties after we switched to the stainless-steel burner. Overall, the flame profiles were very similar using the two burners, but we did observe some consistent differences. In measurements of nascent C_2 profiles using 517-nm LIF detection (e.g., the profile represented by the circles in Fig. 8), the peaks of the profiles measured in acetylene flames were consistently 1–2 mm closer to the burner using the bronze burner compared to using the stainless-steel burner. In measurements of the electronically excited UV-created C_2 profiles (e.g., triangles and squares in Fig. 8), the peaks of the profiles in acetylene flames were consistently 1–2 mm further from the burner using the bronze burner compared to using the stainless-steel burner. We do not know at this time the cause of these differences, although two possibilities are differences in the thermal properties of the burner materials and differences in catalytic effects of the two materials.

We conducted studies using 266-nm radiation because of the ease of generating high-energy fourth-harmonic output from a Nd:YAG laser. The choice of the 292-nm wavelength was not arbitrary, but was based on its use for three-photon-excited fluorescence measurements of atomic hydrogen in flames [2]. In fact, this study was motivated to a large extent by interference by Swan-band emission in our atomic hydrogen measurements made using this technique [21]. The effect of this interference on measurements of atomic hydrogen in the 25-Torr, equivalence-ratio 2.0 acetylene-oxygen-argon flame using the bronze burner is illustrated in Fig. 10. In this figure, the two profiles are normalized to agree in the post-flame gases (height greater than 30 mm), in which laser-induced Swan-band emission is relatively small (Fig. 8). The profile represented by the circles was measured using two-step fluorescence detection (two-photon $1S$–$2S$ excitation

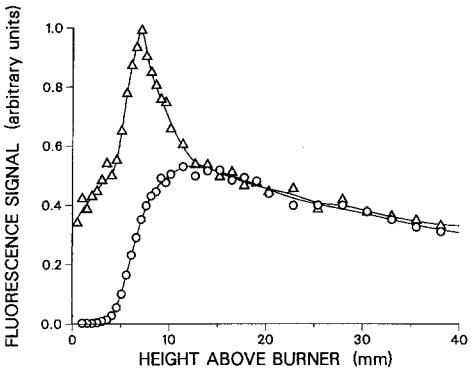

Fig. 10. Profiles of atomic hydrogen LIF signals recorded in the 25-Torr, equivalence-ratio 2.0 acetylene-oxygen-argon flame stabilized on the bronze burner using three-photon excitation with 20-mJ, 292-nm laser pulses focused by a 25-cm focal length lens and Spex spectrometer detection (squares), and using two-step excitation (circles). The profiles have been normalized to match in the region 15–40 mm above the burner

using 243-nm radiation followed by single-photon $2S$–$3P$ excitation using 656-nm radiation, and subsequent detection of 656-nm $3P$–$2S$ fluorescence emission) [34]. The profile represented by the triangles was measured using three-photon, 292-nm excitation of the atomic hydrogen $1S$–$4P$ transition, followed by fluorescence detection of 486-nm $4P$–$2S$ emission. The transition was excited using a 25-cm focal-length lens to focus 20-mJ pulses into the flame, and monitoring the resulting emission using the Spex spectrometer set at 486 nm.

Our experience in measuring atomic hydrogen concentration profiles in flames using three fluorescence detection techniques (two-photon 205-nm excitation [35], in addition to the two-step and three-photon methods) indicates that the two-step measurement best represents the true profile of atomic hydrogen in the flame [21]. The three-photon-excitation profile in Fig. 10 differs from the two-step profile primarily in two ways, namely the presence of a very sharp peak at approximately 7 mm above the burner, and the presence of a relatively large signal very close to the burner surface (before the reaction zone of the flame). These differences were observed consistently in the rich acetylene flames that we studied. The former is consistent with the height of the laser-excited Swan-band emission peak in Fig. 8 (recorded in the same flame), and suggests that the small amount of Swan-band emission at 486 nm (Fig. 1) is simply passing through the spectrometer and interfering with the measurement of the very weak atomic hydrogen fluorescence. Laser-induced Swan-band emission could also be responsible for the relatively large signal near the burner surface, although we did not observe such a large signal (relative to the signal at the peak of the profile) in our direct C_2 studies in rich acetylene flames (e.g., the measurements shown in Fig. 8). Measurements made with the laser tuned just off the atomic hydrogen three-photon transition indicate that a portion of the excess signals observed in the region 0–15 mm above the burner is due to photochemical creation of atomic hydrogen [28, 29] from the photolysis of the gases in the preheat and reaction zones of the flame. We have not yet determined the relative contributions of these two effects (laser-induced Swan-band emission and photochemical formation of atomic hydrogen), but we have determined that both are contributing to the differences in the profiles shown in Fig. 10. Their relative magnitude depends strongly on the bandwidth of the detection system; a higher-resolution spectrometer more successfully discriminates against the relatively broadband Swan-band emission, without discriminating against the narrow-band atomic hydrogen emission. Unfortunately, higher resolution is generally obtained with some loss in spectrometer transmission, leading to decreased detection efficiency of the already-weak atomic hydrogen signal.

6. Conclusion

We have described the characteristics of C_2 creation and Swan-band emission in a variety of environments relevant to laser-based diagnostics, and combustion diagnostics in particular. The topics treated include C_2 spectroscopy, emission lifetimes and quenching in room-temperature acetylene and ethylene flows, intensity dependences in room-temperature flows and in flames, profiles of a-state C_2 and laser-created Swan-band emission in flames, and the effect of laser-created Swan-band emission on three-photon-excited fluorescence detection of atomic hydrogen in flames.

The exact mechanisms responsible for the Swan-band emission are difficult to determine, and evidently vary with wavelength and target gas (or, in flames, with position in the flame). The mechanisms are multi-photon in nature for wavelengths $\geqq 266$ nm in acetylene, ethylene, and the preflame regions of acetylene and ethylene flames, but may be single-photon in the complex mixture of gases in the reaction zones of some flames. Regardless of the mechanisms involved, however, Swan-band emission is a likely result any time that intense laser pulses of almost any wavelength are focused into carbon-containing gases. Because this emission spans much of the visible region of the spectrum, it can interfere with fluorescence detection of many atomic and molecular species, and can adversely affect a wide range of laser-based diagnostic techniques.

References

1. A.G. Gaydon: *The Spectroscopy of Flames*, 2nd. edn. (Chapman and Hall, London 1974)
2. M. Aldén, A.L. Schawlow, S. Svanberg, W. Wendt, P.-L. Zhang: Three-photon excited fluorescence detection of atomic hydrogen in an atmospheric-pressure flame. Opt. Lett. **9**, 211 (1984)
3. C.J. Vear, P.J. Hendra, J.J. Macfarlane: Laser Raman and resonance fluorescence spectra of flames. J. Chem. Soc. (London) Chem. Comm. **7**, 381 (1972)
4. K.H. Becker, D. Haaks, T. Tatarczyk: Measurements of C_2 radicals in flames with tunable dye-laser. Z. Naturforsch. **29a**, 829 (1974)
5. A.P. Baronavski, J.R. McDonald: Measurement of C_2 concentrations in an oxygen-acetylene flame: An application of saturation spectroscopy. J. Chem. Phys. **66**, 3300 (1977)
6. A.P. Baronavski, J.R. McDonald: Application of saturation spectroscopy to the measurement of C_2, $^3\Pi_u$ concentrations in oxy-acetylene flames. Appl. Opt. **16**, 1897 (1977)
7. S.J. Harris, A.M. Weiner: Intracavity laser tomagraphy of C_2 in an oxyacetyle flame. Opt. Lett. **6**, 434 (1981)
8. J.A. Vanderhoff, R.A. Beyer, A.J. Kotlar, W.R. Anderson: Ar^+ laser excited fluorescence of C_2 and CN produced in a flame. Combust. Flame **49**, 197 (1983)
9. M. Aldén, H. Edner, S. Svanberg: Simultaneous, spatially resolved monitoring of C_2 and OH in a C_2H_2/O_2 flame using a diode array detector. Appl. Phys. B **29**, 93 (1982)
10. R.W. Dibble, M.B. Long, A. Masri: Two-dimensional imaging of C_2 in turbulent nonpremixed jet flames. In *Dynamics of Reactive Systems Part II: Modeling and Heterogeneous Combustion*, ed. by J.R. Bowen, J.-C. Leyer, R.I. Soloukhin, *Progress in Astronautics and Aeronautics* **105** (American Institute of Aeronautics and Astronautics, New York 1986) pp. 99–109
11. M.G. Allen, R.D. Howe, R.K. Hanson: Digital imaging of reaction zones in hydrocarbon-air flames using planar laser-induced fluorescence of CH and C_2. Opt. Lett. **11**, 126 (1986)
12. B. Attal, D. Débarre, K. Müller-Dethlefs, J.P.E. Taran: Resonance-enhanced coherent anti-Stokes Raman scattering in C_2. Rev. Phys. Appl. **18**, 39 (1983)
13. D.A. Greenhalgh: RECLAS: Resonant enhanced CARS from C_2 produced by laser ablation of soot particles. Appl. Opt. **22**, 1128 (1983)
14. J.A. Howe: Observations on the maser-induced graphite Jet. J. Chem. Phys. **39**, 1362 (1963)
15. M.H. Yu, M.R. Levy, C. Wittig: The production of $CN(X^2\Sigma^+)$ and $C_2(A^3\Pi_u)$ via the infrared multiple photon dissociation of C_2H_3CN. J. Chem. Phys. **72**, 3789 (1980)
16. J.R. McDonald, A.P. Baronavski, V.M. Donnelly: Multiphoton-vacuum-ultraviolet laser photodissociation of acetylene: Emission from electronically excited fragments. Chem. Phys. **33**, 161 (1978)
17. A.C. Eckbreth: Effects of laser-modulated particulate incandescence on Raman scattering diagnostics. J. Appl. Phys. **48**, 4473 (1977)
18. M. Aldén, S. Wallin, W. Wendt: Applications of two-photon absorption for detection of CO in combustion gases. Appl. Phys. B **33**, 205 (1984)
19. K.C. Smyth, J.H. Miller, R.C. Dorfman, W.G. Mallard, R.J. Santoro: Soot inception in a methane/air diffusion flame as characterized by detailed species profiles. Combust. Flame **62**, 157 (1985)
20. A.R. Masri, R.W. Bilger, R.W. Dibble: Fluorescence interference with Raman measurements in nonpremixed flames of methane. Combust. Flame **68**, 109 (1987)
21. J.E.M. Goldsmith: Multiphoton-excited fluorescence measurements of atomic hydrogen in low-pressure flames, in *Twenty-Second Symposium (International) on Combustion* (The Combustion Institute, Pittsburgh, PA 1989) pp. 1403–1411
22. See, for example, G. Herzberg: *Molecular Spectra and Molecular Structure. I. Spectra of Diatomic Molecules*, 2nd edn. (Van Nostrand Reinhold, New York 1950) p. 454
23. K.P. Huber, G. Herzberg: *Molecular Spectra and Molecular Structure. IV. Constants of Diatomic Molecules* (Van Nostrand Reinhold, New York 1979) p. 114
24. W.L. Faust, L.S. Goldberg, B.B. Craig, R.G. Weiss: Time-resolved C_2 Swan emission from short-pulse UV fragmentation of CO: Evidence for two C_2 formation mechanisms. Chem. Phys. Lett. **83**, 265 (1981), and references therein
25. C. Naulin, M. Costes, G. Dorthe: C_2 radicals in a supersonic molecular beam radiative lifetime of the $d^3\Pi_g$ state measured by laser-induced fluorescence. Chem. Phys. Lett. **143**, 496 (1988) and references therein
26. P. Erman: The influence of collisional transfer effects on measured C_2 swan band transition probabilities. Phys. Scr. **22**, 108 (1980)
27. C.T. Lin, Ph. Avouris, Y.J. Thefaine: Photolysis wavelength dependence of the effect of Xenon on the production of $C_2^*(d^3\Pi_g)$ by ultraviolet multiphoton dissociation. J. Phys. Chem. **86**, 2271 (1982)
28. J.E.M. Goldsmith: Photochemical effects in 205-nm, two-photon-excited fluorescence detection of atomic hydrogen in flames. Opt. Lett. **11**, 416 (1986)
29. J.E.M. Goldsmith: Photochemical effects in 243-nm two-photon excitation of atomic hydrogen in flames. Appl. Opt. **28**, 1206 (1989)
30. J.E.M. Goldsmith: Photochemical effects in two-photon-excited fluorescence detection of atomic oxygen in flames. Appl. Opt. **26**, 3566 (1987)
31. H. Okabe, R.J. Cody, J.E. Allen, Jr.: Laser photolysis of C_2H_2 and CF_3C_2H at 193 nm: Production of $C_2(d^3\Pi_g)$ and $CH(A^2\Delta)$ and their quenching by Xe. Chem. Phys. **92**, 67 (1985)
32. V.M. Donnelly, L. Pasternack: Reactions of $C_2(a^3\Pi_u)$ with CH_4, C_2H_2, C_2H_6, and O_2 using multiphoton UV excimer laser photolysis. Chem. Phys. **39**, 427 (1979)
33. A.M. Wodtke, Y.T. Lee: Photodissociation of acetylene at 193.3 nm. J. Phys. Chem. **89**, 4744 (1985)
34. J.E.M. Goldsmith: Two-step saturated fluorescence detection of atomic hydrogen in flames. Opt. Lett. **10**, 116 (1985)
35. R.P. Lucht, J.T. Salmon, G.B. King, D.W. Sweeney, N.M. Laurendeau: Two-photon excited fluorescence measurement of hydrogen atoms in flames. Opt. Lett. **8**, 365 (1983)